# Mechanistic Investigation of the Nickel-Catalyzed Metathesis between Aryl Thioethers and Aryl Nitriles



**Author(s):**
Boehm, Philip; Müller, Patrick; Finkelstein Dobratz, Patrick; Rivero Crespo, Miguel Ángel; Ebert, Marc-Olivier; Trapp, Nils; Morandi, Bill

**Publication date:**
2022-07-27

**Permanent link:**
https://doi.org/10.3929/ethz-b-000562718



**Originally published in:**
Journal of the American Chemical Society 144(29), https://doi.org/10.1021/jacs.2c01595

**Funding acknowledgement:**
184658 - Catalytic synthesis of unprotected amines and heterocycles (SNF)
757608 - Shuttle Catalysis for Reversible Molecular Construction (EC)

# Mechanistic Investigation of the Nickel-Catalyzed Metathesis between Aryl Thioethers and Aryl Nitriles

Philip Boehm,‡ Patrick Müller,‡ Patrick Finkelstein, Miguel A. Rivero-Crespo, Marc-Olivier Ebert, Nils Trapp and Bill Morandi*

*ETH Zürich, Vladimir-Prelog-Weg 3, HCI, 8093 Zürich, Switzerland*

**ABSTRACT:** Functional group metathesis is an emerging field in organic chemistry with promising synthetic applications. However, no complete mechanistic studies of these reactions have been reported to date, particularly regarding the nature of the key functional group transfer mechanism. Unravelling the mechanism of these transformations would not only allow for their further improvement, but would also lead to the design of novel reactions. Herein, we describe our detailed mechanistic studies of the nickel-catalyzed functional group metathesis reaction between aryl methyl sulfides and aryl nitriles combining experimental and computational results. These studies did not support a mechanism proceeding through reversible migratory insertion of the nitrile into a Ni–Ar bond, and provided strong support for an alternative mechanism involving a key transmetalation step between two independently generated oxidative addition complexes. Extensive kinetic analysis, including rate law determination and Eyring analysis indicated the oxidative addition complex of aryl nitrile as the resting state of the catalytic reaction. Depending on the concentration of aryl methyl sulfide, either the reductive elimination of aryl nitrile or the oxidative addition into the C($sp^2$)–S bond of aryl methyl sulfide are the turnover-limiting steps of the reaction. NMR studies, including an unusual $^{31}P$-$^{2}H$ HMBC experiment using deuterium-labeled complexes, unambiguously demonstrated that the sulfide and cyanide groups exchange during the transmetalation step, rather than the two aryl moieties. In addition, Eyring and Hammett analysis of the transmetalation between two Ni(II) complexes revealed that this central step proceeds via an associative mechanism. Organometallic studies involving the synthesis, isolation and characterization of all putative intermediates and possible deactivation complexes have further shed light on the reaction mechanism, including the identification of a key deactivation pathway which has led to an improved catalytic protocol.

## INTRODUCTION

Alkene metathesis is a powerful tool in organic chemistry for the construction and deconstruction of C=C bonds.[1–6] It is widely used in a variety of fields ranging from natural product synthesis[6–8] to materials science.[9] The full mechanistic elucidation of this reaction was key to unlock the development of more active catalysts and further improve the substrate scope (Figure 1A).[1,6,10–12]

In contrast, catalytic functional group metathesis, which proceeds through the exchange of two functional groups *via* reversible cleavage of two single bonds, has only emerged recently as a highly promising strategy in organic synthesis (Figure 1B).[13] The Arndtsen group and our group independently developed a palladium-catalyzed functional group metathesis between aryl iodides and aroyl chlorides.[14,15] Yamaguchi and co-workers have reported the Ni-catalyzed transfer of an ester moiety to a range of aryl halides,[16] and extended this methodology to the transfer of sulfides to different aryl electrophiles.[17] Recently, we have disclosed the Ni-catalyzed metathesis between aryl thioethers and aryl nitriles.[18] The reaction exhibited a broad substrate scope in both aryl nitriles and aryl sulfides, could be used to circumvent the need for hazardous reagents (such as cyanide salts or low-molecular weight thiols), and proved useful in target-oriented synthesis (Figure 1C).

The limited number of reports on functional group metathesis underscores the challenge for further development of this class of reactions. The design of more functional group metathesis reactions will benefit from a greater mechanistic understanding, especially given the need to identify a suitable transfer mechanism to exchange two chemically distinct functional groups. Importantly, this understudied transfer of two functional groups between two complexes of the same transition metal, in particular between two nickel complexes, has broad relevance in catalysis, as it might be involved in several other reactions classes, e.g. cross-electrophile couplings, C–H activation or polymerization reactions.[19–25] Despite numerous reports on transmetalation between two transition metal centers,[14,26,27–33] there is only scattered literature on transmetalation between two nickel centers.[17,34–38] These studies were limited to isolated experiments based either on product detection upon mixing of two complexes,[17,34–36] or on the kinetic observation of second

order in catalyst concentration.[37] Important key questions regarding the transmetalation, most notably whether the aryl groups or the other X-type ligands were exchanged in these reactions, thus remain largely unanswered.

In this work, we report a detailed kinetic and organometallic study of the Ni-catalyzed metathesis between aryl nitriles and aryl thioethers.[18] We used kinetic and spectroscopic analysis to identify the resting state and the turnover-limiting step of this reaction.

Figure 1. Context of this work.

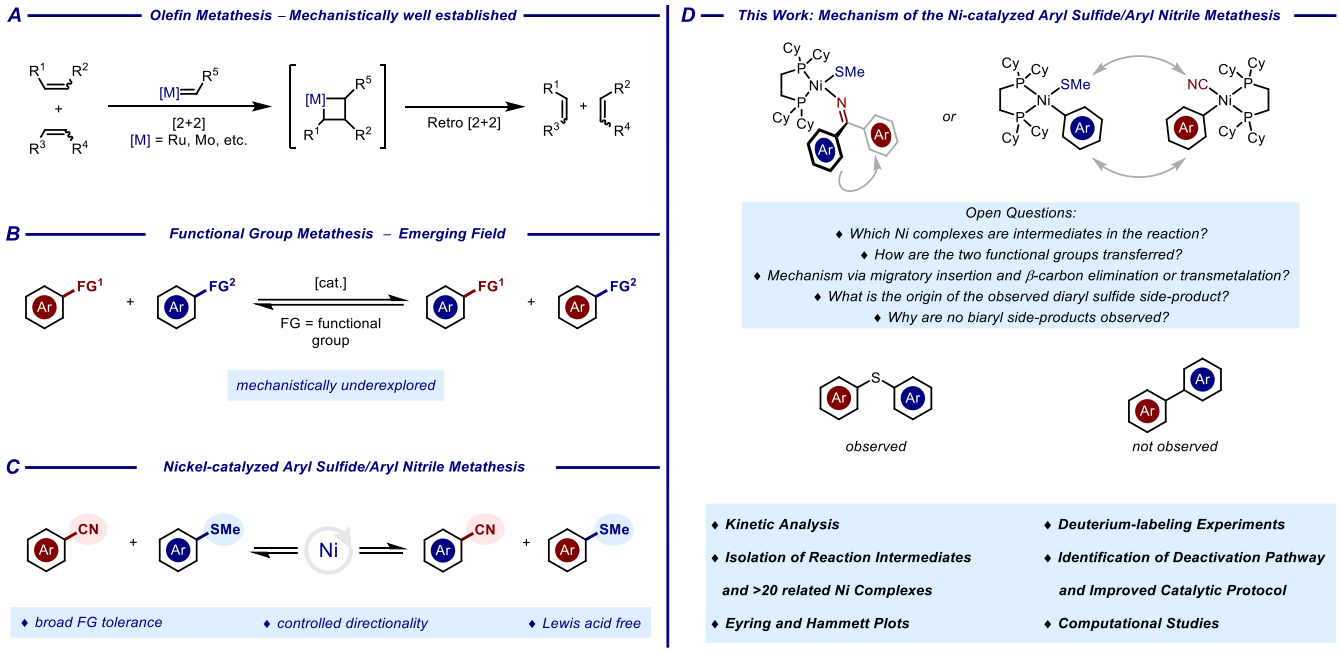


Activation parameters for important steps of the proposed catalytic cycle were determined in stoichiometric organometallic studies and further supported by DFT calculations. Valuable information about the transmetalation step could be obtained by Hammett analysis and by using deuterium-labeled complexes. This accumulated knowledge finally helped us devise a strategy to overcome a newly uncovered deactivation pathway and propose a catalytic cycle that is consistent with our observations (Figure 1D).

## RESULTS AND DISCUSSION

### Mechanistic Hypotheses

At the outset of our studies, we proposed two possible mechanisms based on observations made during reaction development,[18] as well as literature precedent that included a proposed transmetalation between two catalytically active nickel centers (Scheme 1).[17,34–37] A specific consideration related to the reversibility of our reaction is the need for fully symmetrical catalytic cycles, i.e. bonds are formed and cleaved through the same mechanism and transition states, consistent with the microscopic reversibility principle.[39]

Hypothetical mechanism A (Scheme 1) commences with the reported oxidative addition of the dcype-ligated Ni(0) catalyst into the C($sp^2$)–S bond of the aryl methyl sulfide starting material.[40,41] The formed Ni(II) complex next reacts with the C≡N bond of the nitrile substrate through a migratory insertion mechanism. Such migratory insertions of nitriles into Ni(II)–aryl species have been proposed previously, albeit with the assistance of Lewis acids coordinating to the nitrile nitrogen.[42–44] By undergoing the formal reverse reaction of migratory insertion – β-carbon elimination – the formed Ni(II)-iminyl species then releases a new aryl nitrile. The β-carbon elimination step has been extensively studied for rhodium and palladium.[45–51] However, only recently it has been proposed as a potential mechanistic pathway in a Ni-catalyzed reaction.[52] The formed aryl–Ni(II)–SMe complex could then reductively eliminate[40,41] to release the aryl methyl sulfide and close the catalytic cycle. This mechanistic hypothesis was primarily based on the observation of *N*-arylated diarylimine by GC-MS analysis during the optimization of the metathesis reaction.[18]

For hypothetical mechanism B (Scheme 1), independent oxidative additions of the Ni/dcype catalyst into the C–SMe bond of the aryl methyl sulfide and the C–CN bond of the aryl nitrile generate two oxidative addition complexes. These elementary steps are known for either the Ni/dcype- or related catalyst systems.[17,40,41,53–55] In a central transmetalation event between two nickel complexes, either the thiolate and cyanide moieties or the two aryl groups of the two complexes exchange to form the two scrambled Ni(II) complexes.

Similar transmetalation processes have already been proposed for nickel-catalyzed reactions.[17,34–37] Both complexes can then undergo final reductive elimination to regenerate the active Ni(0) catalyst and release both products.

Scheme 1. Plausible proposed mechanisms for the nickel-catalyzed metathesis ([Ni] = [Ni(dcype)] or [Ni(dcype)(cod)]).

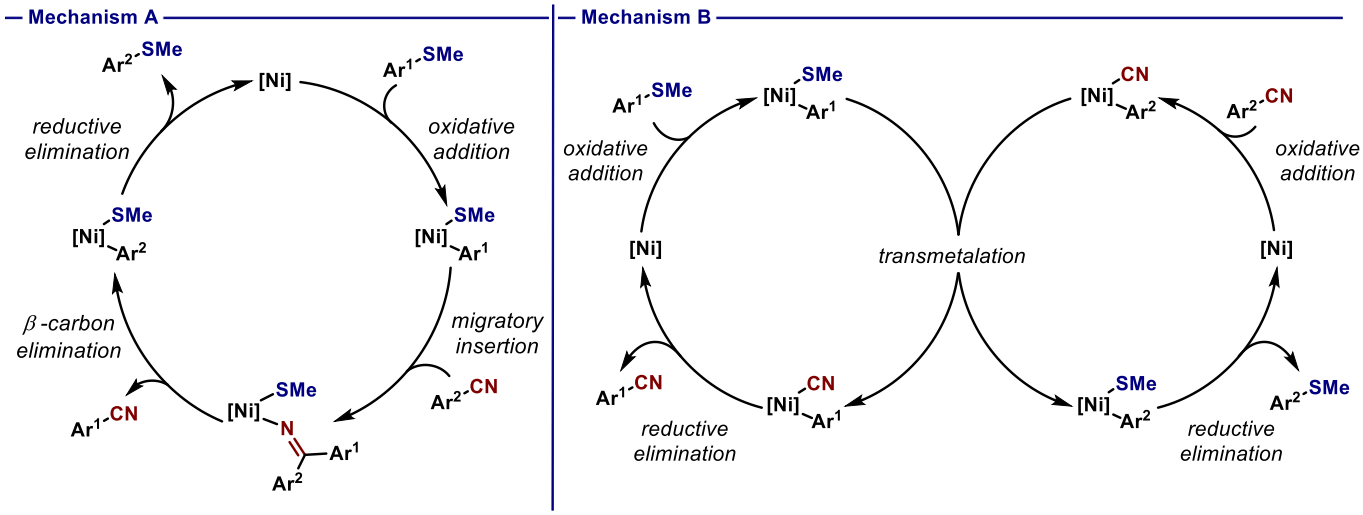


We have chosen a model reaction to study the nickel-catalyzed metathesis between aryl thioethers and aryl nitriles, (Scheme 2). The substrates 4-(trifluoromethyl)benzonitrile (**1**) and 4-methoxythioanisole (**2**) have been selected due to their commercial availability, and the high yield of both products 4-(trifluoromethyl)thioanisole (**3**) and 4-methoxybenzonitrile (**4**) in the previously reported metathesis reaction.[18]

Scheme 2. Model reaction for the functional group metathesis.

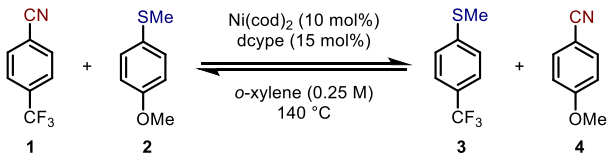


Mechanism involving β-Carbon Elimination

With proposed mechanism A in mind, we commenced our study with the synthesis of the oxidative addition complex of the [Ni(cod)$_2$]/dcype catalyst system into the C(sp$^2$)–S bond of 4-methoxythioanisole (**2**). Similar complexes had been synthesized previously.[40,41] Unfortunately, direct synthesis *via* oxidative addition into the C(sp$^2$)–S bond proved to be challenging due to difficulties during the purification of the complex. We therefore synthesized the oxidative addition complex [Ni(dcype)(ArOMe)(SMe)] (**6**) (ArOMe = *p*-C$_6$H$_4$OMe) *via* a two-step route starting with the oxidative addition of [Ni(cod)$_2$]/dcype into the C–Br bond of 4-methoxybromobenzene (**5**), followed by salt metathesis with sodium thiomethanolate. (Scheme 3A). We then investigated the synthesis of the putative nickel-iminyl intermediate, which might stem from the migratory insertion of the C≡N bond of 4-(trifluoromethyl)benzonitrile (**1**) into the Ni–Ar bond of **6** (Scheme 3B). After deprotonation of the appropriate unsymmetrical diaryl imine with butyl sodium (see SI, chapter 2 for details), we reacted the resulting iminyl sodium **7** with [Ni(dcype)(SMe)$_2$] (**8**) to form Ni-iminyl complex **9**. The identity of **9** was confirmed by single-crystal X-ray and NMR analysis. According to the crystal structure, the C=N bond is in *Z*-configuration, with the Ni-fragment and the *p*-methoxyphenyl group on the same side. The Ni–N–C$_{iminyl}$ angle measures 138.4(3)°. Assuming *syn* addition of the aryl and the nickel fragment during the migratory insertion, free rotation around the Ni–N–C$_{iminyl}$ axis is required for a productive β-carbon elimination. Although the presence of the *E*-isomer could not be detected by $^{31}$P{$^1$H}-NMR spectroscopy, DFT calculations support the possibility of isomerization under our reaction conditions (see SI, chapter 8).

Scheme 3. Synthesis of putative reaction intermediates and probing the key steps of mechanism A.

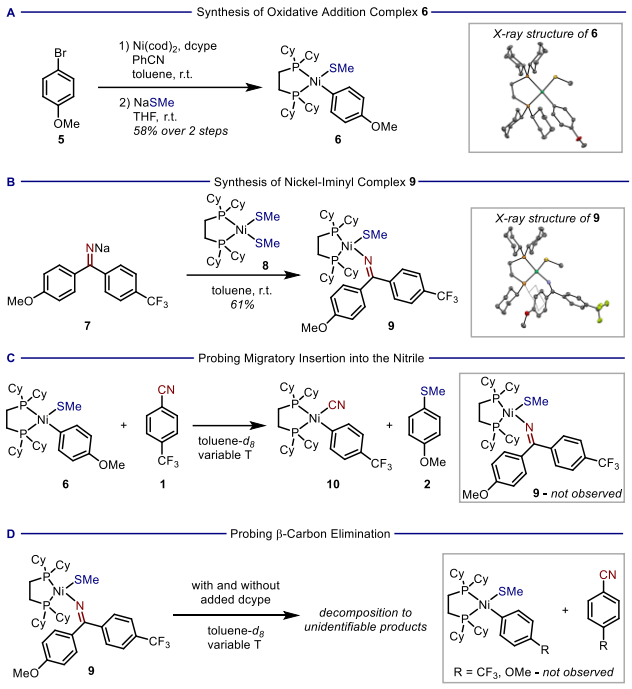


After the successful synthesis of these two nickel-complexes, we stoichiometrically probed the migratory insertion of the C≡N bond of **1** into the Ni–Ar bond of [Ni(dcype)(ArOMe)(SMe)] **6**. We reacted equimolar amounts of **6** with **1** in toluene-$d_8$[56] at different temperatures and monitored the reaction *in situ* by $^1$H- and $^{31}$P{$^1$H}-NMR spectroscopy (Scheme 3C). Instead of observing the signals corresponding to the migratory insertion product **9**, we observed two new sets of doublets in the $^{31}$P{$^1$H}-NMR spectrum, which matched the signals of the oxidative addition complex of 4-(trifluoromethyl)benzonitrile, [Ni(dcype)(ArCF$_3$)(CN)] (**10**) (ArCF$_3$ = *p*-C$_6$H$_4$CF$_3$). When analyzing the reaction mixture by GC-MS, we could also observe free 4-methoxythioanisole (**2**). These results suggest that rather than undergoing migratory insertion of the aryl nitrile C≡N bond, complex **6** reductively eliminates to release **2** and subsequently undergoes oxidative addition into aryl nitrile **1** to form the oxidative addition complex **10**. Similarly, we also probed the β-carbon elimination from Ni-iminyl complex **9** (Scheme 3D). We heated complex **9** in toluene-$d_8$ both with and without additional dcype ligand[41] at different temperatures and followed the reaction by $^1$H- and $^{31}$P{$^1$H}-NMR spectroscopy. We anticipated observing either aryl nitriles **1** or **4** stemming from β-carbon elimination and one of the two corresponding oxidative addition complexes of thioanisole or their reductive elimination products, respectively. Instead, we could only observe a complex mixture of unidentifiable products by NMR analysis. GC-MS analysis of the same reaction mixture only showed the corresponding diaryl ketone resulting from imine hydrolysis. This result indicates that β-carbon elimination from this nickel-iminyl complex does not appear to be accessible under these reaction conditions. In addition, complex **9** proved to be catalytically, but not kinetically competent under the standard reaction conditions (see SI, chapter 4 for details). Collectively, these results show that the reaction is most likely not proceeding *via* a pathway including migratory insertion of the aryl nitrile C≡N bond to form a Ni-iminyl complex and subsequent β-carbon elimination.

## Mechanism involving Transmetalation

### Synthesis of Oxidative Addition Complexes

After showing that mechanism A is most likely not operative under the reaction conditions, we turned our attention towards proposed mechanism B (Scheme 1). Four key hypothetical intermediates are proposed for this mechanism, the two oxidative addition complexes **6** and **10** of the two starting materials **1** and **2**, and the two oxidative addition complexes **11** and **12** of the two products **3** and **4** (Figure 2). Complex **6** had already been synthesized for the investigation of mechanism A; therefore, we focused our efforts on synthesizing the remaining three complexes. The oxidative addition complex of the [Ni(cod)$_2$]/dcype catalyst into the C(sp$^2$)–S bond of 4-(trifluoromethyl)thioanisole (**3**) proceeded smoothly and afforded complex **11** in 93% yield. The oxidative addition of [Ni(cod)$_2$]/dcype into the C–CN bond of aryl nitriles has not been described in literature so far. Jones and co-workers reported the oxidative addition of a related Ni-system with a similarly electron-rich ligand, 1,2-di(*iso*-propylphosphino)ethane (dippe).[53–55] We were able to access complex **10** by direct oxidative addition of [Ni(cod)$_2$]/dcype into the C–CN bond of 4-(trifluoromethyl)benzonitrile (**1**) in 97% yield. Similarly to complex **6**, we were not able to access complex **12** *via* direct oxidative addition into the C–CN bond of 4-methoxybenzonitrile (**2**). Instead, we synthesized **12** in an analogous manner to complex **6**, using tetrabutylammonium cyanide for the salt metathesis. The structures of all complexes were confirmed by single-crystal X-ray and NMR analysis. All four

complexes proved to be kinetically competent under the standard reaction conditions (see SI, chapter 4 for details), supporting their key role in the catalytic cycle.

Figure 2. Synthesized intermediates for proposed mechanism B and their X-ray crystal structures.

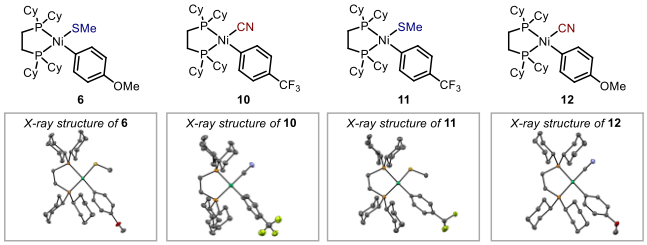


Kinetic Analysis of the Catalytic Reaction

Having synthesized and confirmed the kinetic competence of all the putative intermediates, we performed kinetic analysis of the Ni-catalyzed metathesis between aryl sulfides and aryl nitriles to pinpoint the nature of the resting state and turnover-limiting step, as well as gather information about possible deactivation pathways. When analyzing the reaction progress by gas chromatography, we observed that the standard reaction (Scheme 2) does not exhibit an induction period, but rather a steady increase in product concentration with complete conversion achieved within approximately 5 hours (see SI, chapter 4 for more details). In addition, we noticed minor catalyst deactivation when running same excess experiments, as described by Blackmond.[57,58] We did not detect product inhibition under the same conditions with added products **3** and **4**.

For the determination of the experimental rate law, we used the method of initial rates (up to 15% conversion, see SI chapter 4 for more details). By varying the concentration of the $[Ni(cod)_2]$/dcype-catalyst (0.01875–0.0375 M), we observed a first-order dependence of the rate of the reaction on catalyst concentration (see Figure 3). Furthermore, we observed an inverse first order in aryl nitrile **1** when varying its concentration (0.125–0.375 M). The order in aryl methyl sulfide **2** changed with varying concentrations, revealing a change in the reaction regime. We observed a first order dependence in **2** for low concentrations and a zero-order dependence at higher concentrations. The experimentally-derived rate law from those observations is depicted in Figure 3 and the parameters *a* and *b* were obtained by fitting the experimental data to the kinetic model (see SI, chapter 4 for more details and derivations of the theoretical rate law). Despite the fact that the model is a simplification of the real reaction system, the experimental data fits within the prediction interval of the theoretical model at 95% level of confidence.

Figure 3. Experimental rate equation and comparison of the initial rates of the reactions with different initial concentrations of catalyst, **1** and **2**. The experimental data is shown as scattered dots and the theoretical model including the prediction interval at 95% (2σ) level of confidence as solid lines.

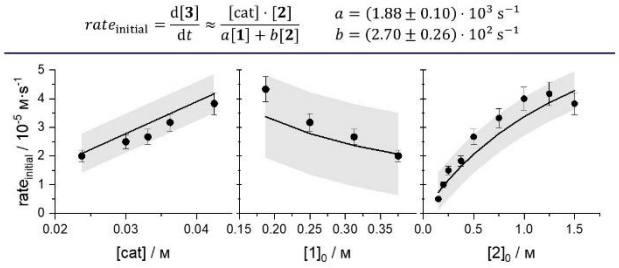


From the inverse first-order dependence on the concentration of **1** and also the *in situ* NMR studies (*vide infra*), we can assume that a nickel-aryl nitrile adduct (with **1** being either coordinated or oxidatively added) is the resting state of the catalyst. The positive order in **2** at low concentrations implies that the oxidative addition into the C($sp^2$)–S bond of **2** occurs before or during the turnover-limiting step of the metathesis reaction. Decoordination of substrate **1** has to occur by ligand exchange with **2**, and this competition for the Ni(0)-intermediate explains the inverse first order in **1**. At higher aryl methyl sulfide concentrations, this step becomes fast enough that the turnover-limiting step shifts to either the reductive elimination or decoordination of **1** from the nickel catalyst.

Eyring Analysis

To gain a deeper insight into the reaction mechanism, Eyring analysis of the oxidative addition/reductive elimination of both aryl nitriles and both aryl methyl sulfides were conducted. The activation parameters were determined in the 60 to 100 °C temperature range by $^1$H-NMR analysis. The oxidative addition and reductive elimination of the aryl nitriles were studied starting from the coordination complex **13** and the oxidative addition complex **12** (Table 1A). At 75 °C, the barriers ($\Delta G^{\ddagger}_{75\ °C}$) for the oxidative additions do not depend on the *para*-substituent of the aryl moiety and are 27 kcal·mol$^{-1}$ in both cases. However, the Gibbs free energy of activation for the reductive elimination step depends on the substituent of the aryl moiety and is smaller for the electron-rich *para*-

methoxyphenyl substituted complex **12** (25 kcal·mol$^{-1}$) compared to the electron-poor trifluoromethyl substituted analogue **10** (28 kcal·mol$^{-1}$). A similar trend was observed in the oxidative addition/reductive elimination reactions of aryl methyl sulfides **2** and **3**. The apparent Gibbs free energy of activation for the oxidative addition starting from [Ni(dcype)(cod)] (**15**) and **2** or **3** is independent of the electronics of the aryl methyl sulfide (24 kcal·mol$^{-1}$ at 75 °C) whereas the apparent Gibbs free energy of activation of the reductive elimination is lower if an electron-rich *para*-methoxyphenyl ligand is present (25 kcal·mol$^{-1}$). In fact, the apparent barrier for the reductive elimination starting from complex **11** was too large to be measured below 100 °C (Table 1B).

To further support the experimental findings and bridge the gap to the catalytic reaction conditions at 140 °C, the relative energies of the different elementary steps for the nitrile reactions were calculated by DFT (Table 1 and SI, chapter 8). The data from the Eyring analysis of the aryl nitriles was used to benchmark a series of different functionals for the electronic energy to determine which one could be used to give the closest values to the experiments. Calculations were run with ORCA 5.0.1[59,60] and all geometries were optimized with the BP86 functional,[61,62] the def2-tzvp(Ni)/def2-svp(other atoms) basis sets,[63] and the D3BJ dispersion correction.[64,65] The PBE0 functional[66] with the def2-qzvp(Ni)/def2-tzvp(other atoms) basis sets and the D3BJ dispersion correction was used for the electronic energy, as this gave the smallest energy differences compared to the experimental values (see SI, chapter 8 for full details). For substrates **13** and **10**, the calculated barriers at 75 °C for the oxidative addition and reductive elimination were 27.3 kcal·mol$^{-1}$ and 28.4 kcal·mol$^{-1}$, respectively, showing a very good agreement with the experimental values. Similarly, for substrate **14** and **12**, the calculated barriers for the oxidative addition and reductive elimination were 27.2 kcal·mol$^{-1}$ and 25.6 kcal·mol$^{-1}$, respectively.

Table 1. Activation parameters of the oxidative addition/reductive elimination of aryl nitriles **1** and **4** and apparent activation parameters for the oxidative addition/reductive elimination of aryl methyl sulfides **2** and **3**.

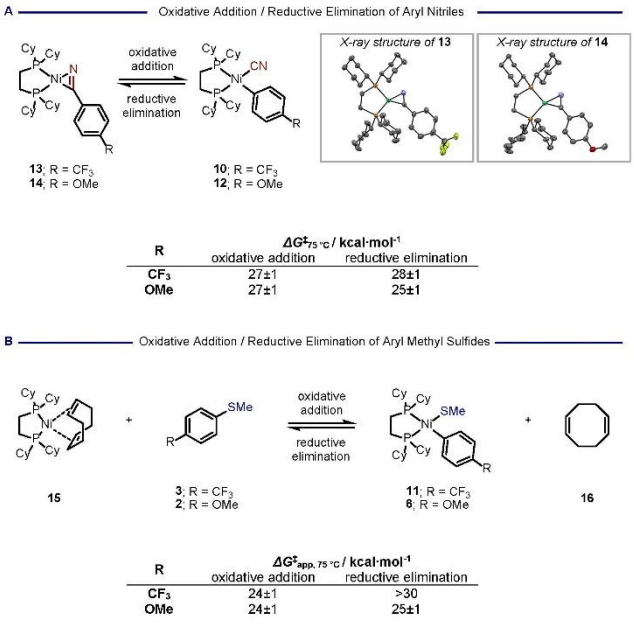


| R | $\Delta G^{\ddagger}_{75\,°C}$ / kcal·mol$^{-1}$ oxidative addition | reductive elimination |
|---|---|---|
| $CF_3$ | 27±1 | 28±1 |
| OMe | 27±1 | 25±1 |

| R | $\Delta G^{\ddagger}_{app,\,75\,°C}$ / kcal·mol$^{-1}$ oxidative addition | reductive elimination |
|---|---|---|
| $CF_3$ | 24±1 | >30 |
| OMe | 24±1 | 25±1 |

Next, the relative energies of the proposed pathway (mechanism B) were computed at 140 °C (Figure 4). In agreement with the observed rate law and based on the computed barriers for the stochiometric reactions, the oxidative addition complex [Ni(dcype)($ArCF_3$)(CN)] (**10**) is proposed as the resting state of the catalytic reaction rather than the coordination complex **13**. The oxidative addition of **2** (29.9 kcal·mol$^{-1}$) is likely to be the turnover-limiting step, in line with the kinetic data. However, due to the low energy difference between the barriers for the oxidative addition into **1** and **2**, the resting state and turnover-limiting step may change during the course of the reaction. Unfortunately, no transition state for the transmetalation could be found (see SI, chapter 8), but experimental data suggests that the barrier is lower than the preceeding steps (*vide infra*). After transmetalation, the two complexes **11** and **12** can both reductively eliminate to release the products of the reaction (both pathways are shown, the nitrile pathway is dashed for clarity). As we had assigned **10** to be the resting state, we proposed that the product release is aided by coordination of another molecule of starting material **1**, i.e. pushing the equilibrium; in both cases leading to the coordinated intermediate **13**. This can then either exchange with starting material **2**, or undergo oxidative addition to participate in the transmetalation.

Figure 4. Calculated Gibbs free energy profile for mechanism B. The optimized transition states for **TS$_{13_10}$** and **TS$_{6coord_6}$** are depictetd.

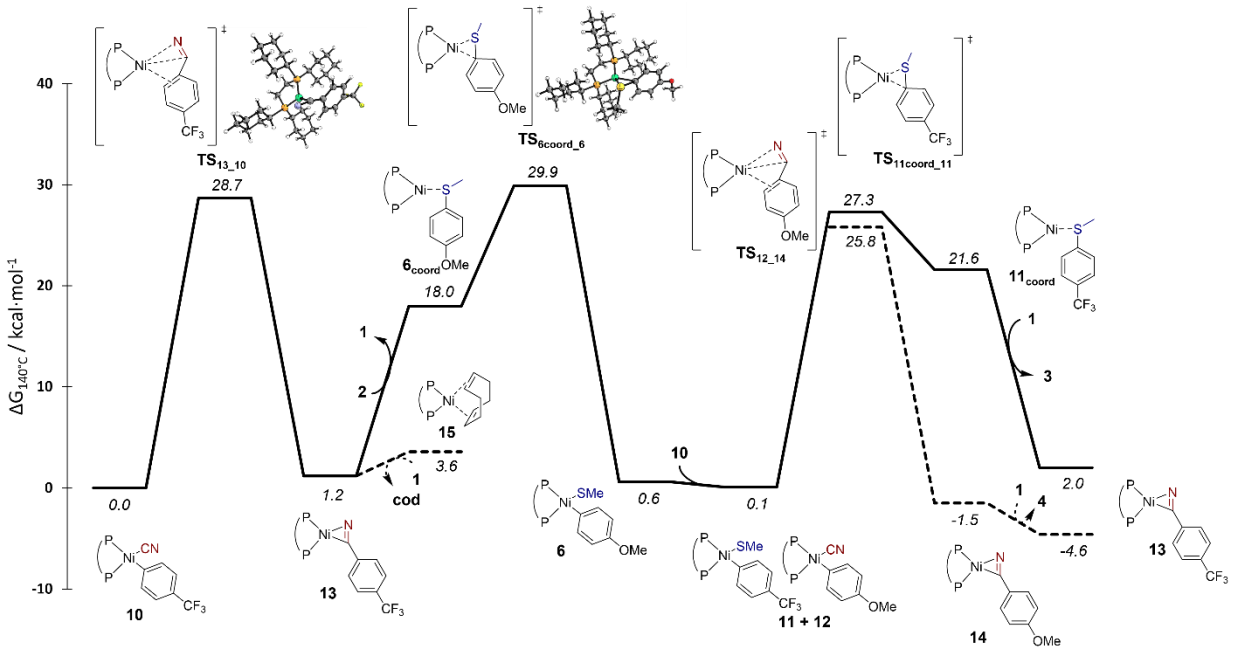


Study of the Transmetalation Step

After studying the two oxidative additions into both the C–CN bond of 4-(trifluoromethyl)benzonitrile (**1**) and into the C(sp$^2$)–S bond of 4-methoxythioanisole (**2**), as well as the two reductive eliminations to form 4-(trifluoromethyl)thioanisole (**3**) and 4-methoxybenzonitrile (**4**), we turned our attention towards the key transmetalation step. In the proposed mechanism B (Scheme 1), a transmetalation between the two oxidative addition complexes **6** and **10** would give the corresponding scrambled complexes **11** and **12**, which would then undergo reductive elimination to release the two products and close the two catalytic cycles. There are only scarce studies of the transmetalation between two nickel oxidative addition complexes,[17,36–39] calling for a careful study of this elementary step.

In a first qualitative experiment, we mixed complexes **6** and **10** in equimolar amounts in toluene-$d_8$ and monitored the reaction *via* $^{31}$P{$^1$H}-NMR analysis (Scheme 4). At 60 °C, we could observe the slow disappearance of the signals at δ = 60.4 ppm and 65.3 ppm (blue dots) and at δ = 63.3 ppm and 74.8 ppm (blue diamonds) of the two starting complexes **6** and **10**, respectively. Concomitantly, we could observe the formation of two new sets of doublets at δ = 60.5 ppm and 65.2 ppm (red dots) and δ = 62.6 ppm and 73.7 ppm (red diamonds), corresponding to the two complexes **11** and **12**, respectively.

Scheme 4. Qualitative transmetalation between complexes **6** and **10** by $^{31}P\{^{1}H\}$-NMR analysis. The intensity of the cyano complexes is low due to their moderate solubility in toluene-$d_8$.

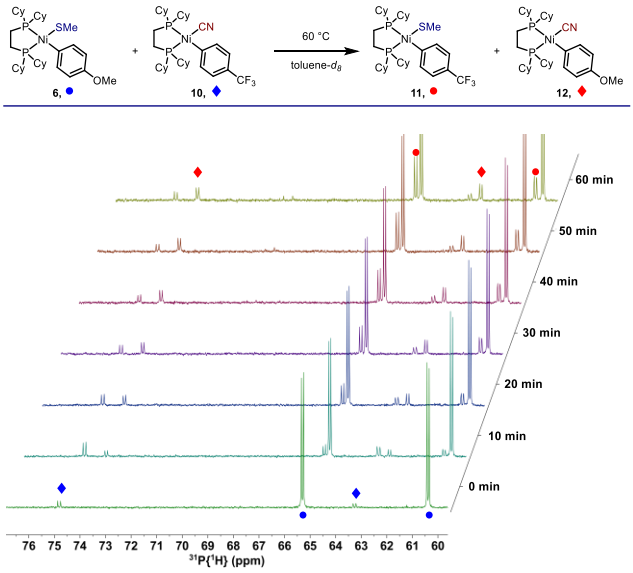


In their recent report, Yamaguchi and co-workers propose that the exchange reaction between aryl electrophiles (esters, carbonates, carbamates and halides) and aryl thioethers proceeds through aryl group exchange.[17] After showing that the transmetalation between the two oxidative addition complexes **6** and **10** proceeds readily, we questioned whether the thiolate and the cyanide, or the two aryl ligands are exchanging in our system. To be able to distinguish between those two options, we synthesized a labeled version of the dcype ligand, containing a deuterated backbone. We anticipated that if mixing a deuterated complex with a non-deuterated complex, we should be able to differentiate *via* $^{31}P\{^{1}H\}$-NMR shifts and $^{31}P$-$^{2}H$-correlation whether a thiolate/cyanide or an aryl group exchange has occurred upon heating. Since direct observation of $^{31}P$-$^{2}H$ splitting ($^{2}J_{PD}$) in the $^{31}P\{^{1}H\}$-NMR spectrum was not possible,[67] we successfully adapted a gradient-selected HMBC experiment to determine which complexes bear a deuterated ligand backbone (see SI, chapter 5). Due to the moderate solubility of the cyano complexes **10** and **12**, we used the oxidative addition complex of 4-phenylthioanisole **17** and the oxidative addition complex of unsubstituted benzonitrile **18** for these model reactions in more polar 1,2-difluorobenzene as solvent.

Starting from labeled complex **17-*d*$_4$**, and non-labeled complex **18**, there are two possible scenarios: 1) if scrambling between the thiolate and the cyanide ligand occurs, complexes **19-*d*$_4$** and **20** should form, with complex **19-*d*$_4$** bearing the deuterated ligand backbone (Scheme 5A), resulting in an emerging cross peak in the $^{31}P$-$^{2}H$-HMBC correlating to the $^{31}P$-NMR signals of complex **19-*d*$_4$**; 2) if scrambling between the two aryl groups occurs instead, complexes **20-*d*$_4$** and **19** should form (Scheme 5B), resulting in an emerging cross peak correlating with the $^{31}P$-NMR signals of complex **20-*d*$_4$**. Before performing the $^{31}P$-$^{2}H$-HMBC experiment, we first performed control experiments to exclude that undesired rapid phosphine ligand scrambling is occurring on the time-scale of our measurements. No significant exchange between the non-deuterated complexes **17** and **18** and dcype-$d_4$ could be detected (see SI, chapter 5), thus indicating that phosphine ligand exchange does not occur to any extent that would deteriorate the results of the $^{31}P$-$^{2}H$-HMBC experiment.

Scheme 5. Differentiation between SMe/CN exchange and aryl group exchange with deuteration pattern after transmetalations.

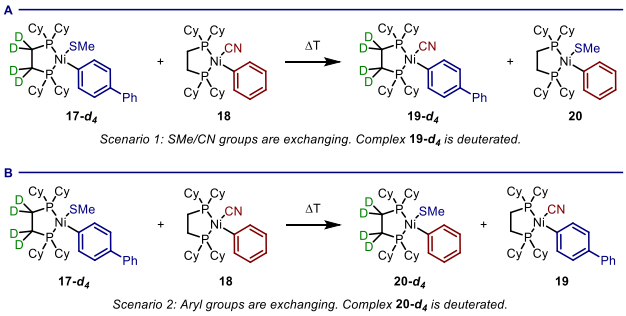


We next performed the transmetalation experiment between complex **17-*d*$_4$** and complex **18** in 1,2-difluorobenzene. Similar to the previous experiment depicted in Scheme 4, we observed new signals in the $^{31}P\{^{1}H\}$-NMR spectrum upon heating to 60 °C, confirming that the transmetalation with the deuterated ligand backbone and the different aryl substituents proceeds smoothly. The results of the $^{31}P$-$^{2}H$-HMBC are depicted in Scheme 6. Initially, there are two cross peaks visible in the $^{31}P$-$^{2}H$-HMBC spectrum, corresponding to

the two phosphorus nuclei of the dcype-$d_4$ ligand of complex **17-*d*$_4$** correlating to the deuterium nuclei of the ligand backbone (Scheme 6A). After approximately 2 hours at 60 °C, two additional signals become visible, indicating the presence of another complex with deuterated ligand backbone (Scheme 6B). The diagnostic chemical shifts of the two doublets in the $^{31}P\{^{1}H\}$-NMR spectrum indicate that this complex bears a cyanide ligand, clearly showing that the predominant pathway proceeds through cyanide/thiolate rather than aryl group exchange. The inherent low propensity of these complexes to transfer aryl groups (over cyanide and thiolato groups) might also explain why biaryl coupling products were not observed under either stoichiometric or catalytic conditions. This selectivity thus effectively prevents an otherwise possible catalyst decomposition through a cross-electrophile coupling pathway that would lead to biaryl formation and presumably inactive [Ni(dcype)$X_2$] complexes.[19–27]

Scheme 6. Indication of SMe/CN exchange in the $^{31}P$-$^{2}H$-HMBC experiment of the transmetalation. The intensity of the thiolato complexes is low due to their moderate solubility in 1,2-difluorobenzene. In spectrum B small additional peaks (74.1, 65.0, 63.1, 61.0 ppm) are visible that arise from slow side reactions. For example, the Ni(II) complexes can undergo reductive elimination under the reaction conditions. Exchange of the ArCN, resp the ArSMe ligands followed by oxidative addition, results in a formal scrambling of dcype and dcype-$d_4$. As the transmetalation is significantly faster than this side reactions, the outcome of the experiment is not affected by it.

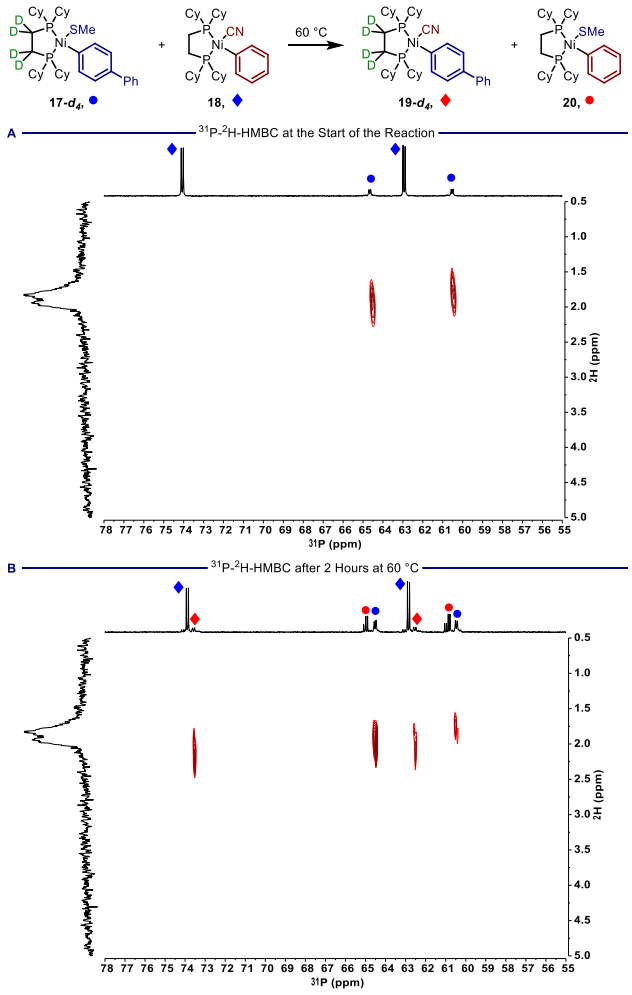


To gain further insight into the mechanism of transmetalation between the two nickel species, the orders in cyano complex **10** and methylthiolato complex **6** were determined (see SI, chapter 5). A first-order dependence in **6** and **10**, indicative of an associative mechanism, was observed. After having established that a cyanide/thiolate exchange is occurring, we wanted to probe the effect of electronics on the transmetalation step. A Hammett analysis was performed by varying the electronic properties of the aryl moiety. Two model reactions were investigated; [Ni(dcype)(ArOMe)(SMe)] (**6**) was reacted with differently substituted cyano complexes **10**, **18** and **19**; and [Ni(dcype)($ArCF_3$)(CN)] (**10**) was reacted with methylthiolato complexes **6**, **17** and **20**, respectively. The rate constants of the reactions were obtained by $^{31}P\{^{1}H\}$-NMR spectroscopy at 70 °C in 1,2-difluorobenzene. The data shows that the rate of transmetalation is affected by substituents that can donate or withdraw electron density through resonance. An enhanced rate can be measured when electron-withdrawing substituents on the aryl ligand of the cyano complex are present, since a π-acceptor ligand (CN) is exchanged by a π-donor ligand (SMe). For the same reason, an enhanced rate is observed when electron-donating substituents are present on the aryl group of the methylthiolato complex (see SI, chapter 5). Under similar conditions as for the Hammett study, the apparent activation parameters for the transmetalation between [Ni(dcype)($ArCF_3$)(CN)] (**10**) and [Ni(dcype)(ArOMe)(SMe)] (**6**)

were determined in the temperature range of 50 °C to 70 °C (Scheme 7). The apparent entropy of activation was found to be highly negative (-29±5 cal·mol$^{-1}$·K$^{-1}$), which further supports an associative mechanism. Based on these collective results, we surmise that the transmetalation step is proceeding through the bimolecular exchange of the cyanide and thiolate ligands through an associative transition state. Unfortunately, no suitable transition state could be located by computational studies.

Scheme 7. Eyring study of the transmetalation.

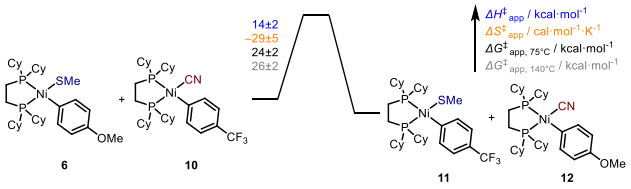


Based on these experimentally determined apparent activation parameters, the Gibbs free energy of activation ($\Delta G^{\ddagger}_{140\,^{\circ}C}$) of the transmetalation at 140 °C, which is the temperature of the catalytic reaction, was calculated to be 26±2 kcal·mol$^{-1}$ using the Gibbs-Helmholtz equation. Since the barrier for transmetalation relative to the proposed resting state is still smaller than for the computed steps (Figure 4), it is unlikely that the transmetalation is the turnover-limiting step of the reaction. Furthermore, the observed order in catalyst (first order) is not in agreement with a turnover-limiting transmetalation step, as in such a scenario a second order dependence is expected. This result together with the other experimental evidence points towards the oxidative addition of the Ni/dcype-catalyst into the C(sp$^2$)–S bond of aryl methyl sulfide **2** as turnover-limiting step.

*In situ* NMR Analysis and Improved Protocol for the Metathesis between Aryl Sulfides and Aryl Nitriles

We continued our mechanistic investigation of the nickel-catalyzed metathesis between aryl thioethers and aryl nitriles with *in situ* NMR analysis of the catalytic reaction. The standard reaction was run in *o*-xylene-$d_{10}$, and was monitored by $^{1}$H- and $^{31}$P{$^{1}$H}-NMR spectroscopy at 140 °C (see SI, chapter 5 for details and spectra). By comparison of the chemical shifts and the coupling constants of the signals in the $^{31}$P{$^{1}$H}-NMR spectrum with the $^{31}$P{$^{1}$H}-NMR spectra of the synthesized samples, we could identify the oxidative addition complex of 4-(trifluoromethyl)benzonitrile [Ni(dcype)(ArCF$_3$)(CN)] (**10)** as a dominant species under catalytic reaction conditions, further supporting our hypothesis that **10** is the catalyst resting state. Apart from the oxidative addition complex **10**, we could also observe the two thioanisole oxidative addition complexes **6** and **11**. However, the *in situ* NMR studies of the Ni-catalyzed metathesis reaction revealed more signals observable in the $^{31}$P{$^{1}$H}-NMR spectrum at 140 °C than originally anticipated. In addition, we observed the formation of undesired organic side-products, such as diaryl sulfides **21**, **22** and **23** (Figure 5) by GC-MS. Additional side-reactions were also observed during the Eyring study of the oxidative addition of the nickel catalyst into the aryl methyl sulfides **2** and **3**. These observations, combined with the results from the kinetic analysis (*vide supra*) indicate that an undesired deactivation pathway is occurring under the reaction conditions. We therefore set out to understand this deactivation pathway and develop an improved protocol for the Ni-catalyzed metathesis between aryl nitriles and aryl sulfides.

Figure 5. Deactivation products observed by GC-MS analysis.

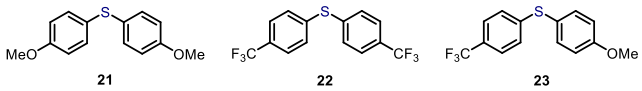


After studying the $^{1}$H-NMR, the $^{31}$P{$^{1}$H}-NMR and the $^{1}$H-$^{31}$P-HMBC NMR spectra of the reaction mixture, we observed upfield shifted signals in the $^{1}$H-NMR spectrum that might correspond to a methyl group bound to the nickel-center (see SI, chapter 5 for details).[68–71] We hypothesized that these complexes might originate from undesired oxidative addition of the Ni/dcype-catalyst into the C(sp$^3$)–S bond of the aryl methyl sulfide starting material, forming complex **24** (Scheme 8).[72–74] Similar to the SMe- and the CN-groups, the arylthiolato group can then likely exchange with other complexes such as **10** to form complexes **25** and **26**. Complex **25** can then undergo reductive elimination to form diaryl sulfide **23**, which was observed as a side-product.

Scheme 8. Potential Deactivation Pathway.

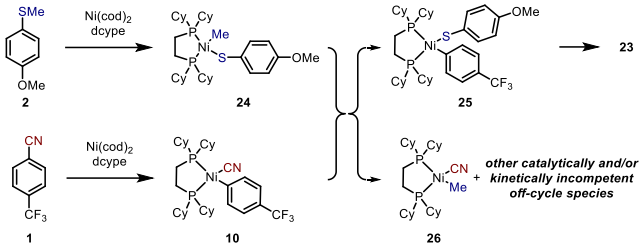


To mechanistically support our hypothesis of catalyst deactivation through formation of Ni–Me complexes, we set out to independently synthesize all contemplable Ni-complexes to compare their analytical data with the data we obtained from the *in situ* NMR studies (see SI, chapter 5 for details). Eventually, we could identify the major signals as the already assigned productive intermediates **6**, **10**, and **11**. In addition to complexes **24** and **26**, we were also able to observe complexes **27** and **28** by comparison of the $^{31}P\{^{1}H\}$-NMR shifts and the coupling constants (Figure 6, see SI, chapter 5 for details). This result supports the hypothesis that undesired oxidative addition into the C($sp^3$)–S bond of 4-methoxythioanisole (**2**) and subsequent ligand exchange with other complexes present in the reaction mixture is occurring under the reaction conditions. Even though the barrier for oxidative addition into the C($sp^3$)–S bond is significantly higher compared to the barrier for oxidative addition into the C($sp^2$)–S bond, DFT calculations support that this step is generally accessible (see SI, chapter 8). Since all the identified complexes (**24**, **26**, **27** and **28**) are catalytically and/or kinetically incompetent under the standard reaction conditions, we assume that those species are the major deactivation complexes.

Figure 6. Identified unproductive complexes in the reaction mixture.

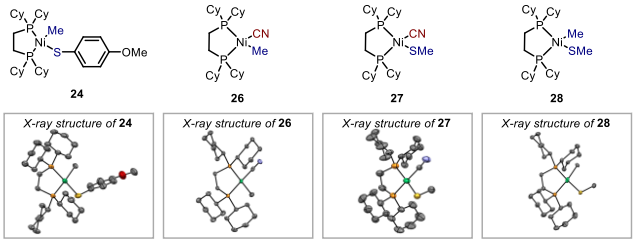


The identification of the oxidative addition into the C($sp^3$)–S bond as side-reaction also explains the presence of diaryl sulfides as sole organic side-products, whereas biaryls were not observed. The diaryl sulfides might originate from oxidative addition into the C($sp^3$)–S bond of the aryl methyl sulfides, subsequent ligand exchange and reductive elimination.

After identification of the deactivation pathway in the nickel-catalyzed metathesis between aryl thioethers and aryl cyanides, we harnessed this knowledge to suppress the undesired oxidative addition into the C($sp^3$)–S bond of the 4-methoxythioanisole (**2**) starting material. We envisioned that if the undesired oxidative addition is blocked by increased steric bulk on the thioether, selective oxidative addition into the desired C($sp^2$)–S bond should occur. Therefore, we synthesized three new aryl alkyl sulfides with a *tert*-butyl, an isopropyl and a neopentyl substituent. Those substrates were then tested under the standard catalytic reaction conditions.

The *tert*-butyl substrate did not afford any product and only starting material was observed by gas chromatography. Excess steric bulk possibly prevents the oxidative addition into both C–S bonds. The isopropyl and the neopentyl substrate **29** and **30**, on the other hand, gave 95% of aryl sulfide **31** and quantitative yield of aryl sulfide **32**, respectively (Scheme 9A). This is a substantial increase compared to the 86% yield reported for the corresponding methyl-substrate **3**.[18] Additionally, no diaryl sulfide products **21**, **22** or **23** were observed by GC-MS analysis. We attribute this increased yield and the absence of side products to the increased steric bulk of the alkyl group at the sulfur, which still allows for oxidative addition into the C(aryl)–S bond, while preventing unproductive oxidative addition into the C($sp^3$)–S bond. When running the reaction for a longer time (72 hours), the catalyst loading could be reduced to 5 mol% nickel instead of the original 10 mol%, with only a minor decrease in yield. The isopropyl substrate afforded the desired exchanged product **31** in 87% yield, the neopentyl substrate gave 91% yield of the scrambled product **32** (Scheme 9B). In comparison, the original methyl-substituted substrate **2** gave a reduced 76% yield of **3** when running the reaction with 5 mol% catalyst loading for 72 hours.

Scheme 9. Improved protocol for the Ni-catalyzed metathesis between aryl sulfides and aryl nitriles. Yields obtained by GC-FID with *n*-dodecane as internal standard.

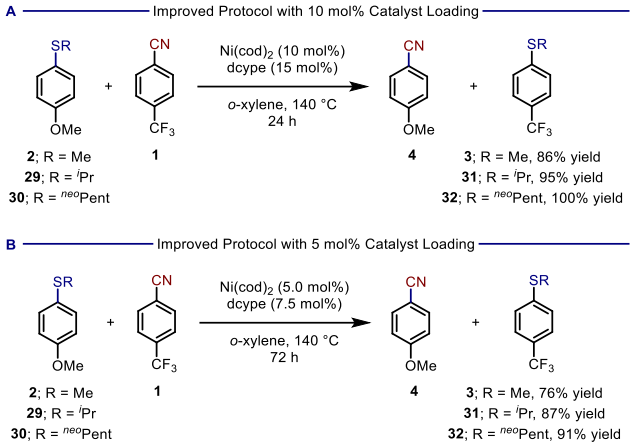


Proposed Catalytic Cycle

On the basis of the combined results from the kinetic analysis, the organometallic studies, the *in situ* NMR experiments and DFT studies, we propose the following catalytic cycle for the nickel-catalyzed functional group metathesis between aryl sulfides and aryl nitriles (Scheme 10). By kinetic analysis (initial rate studies and Eyring analysis) and *in situ* NMR studies, we were able to identify [Ni(dcype)($ArCF_3$)(CN)] (**10**) as the resting state of the catalytic reaction. Kinetic analysis also revealed that if the concentration of aryl methyl sulfide **2** is high, the reductive elimination of aryl nitrile **1** from the Ni(II) resting state is the turnover-limiting step. In contrast, at low concentrations of **2**, the oxidative addition into the $C(sp^2)$–S bond to form [Ni(dcype)(ArOMe)(SMe)] (**6**) becomes turnover-limiting. These results are supported by DFT calculations, showing a small energetic difference in the barriers of the two aforementioned steps, further indicating that a switch in the turnover-limiting step can easily occur by changes in the concentrations. By *in situ* NMR studies and independent synthesis of the complexes, we were able to identify the undesired oxidative addition into the $C(sp^3)$–S bond of the aryl methyl sulfide as a deleterious deactivation pathway. After oxidative addition, transmetalation between [Ni(dcype)(ArOMe)(SMe)] (**6**) and [Ni(dcype)($ArCF_3$)(CN)] (**10**) occurs through exchange of the SMe and CN ligands, as determined by $^{31}P$-$^{2}H$-HMBC experiments using deuterium-labeled complexes. The two scrambled complexes [Ni(dcype)($ArCF_3$)(SMe)] (**11**) and [Ni(dcype)(ArOMe)(CN)] (**12**) can then reductively eliminate to afford both products **3** and **4**.

Scheme 10. Proposed mechanism for the nickel-catalyzed metathesis between aryl sulfides and aryl nitriles based on the obtained results.

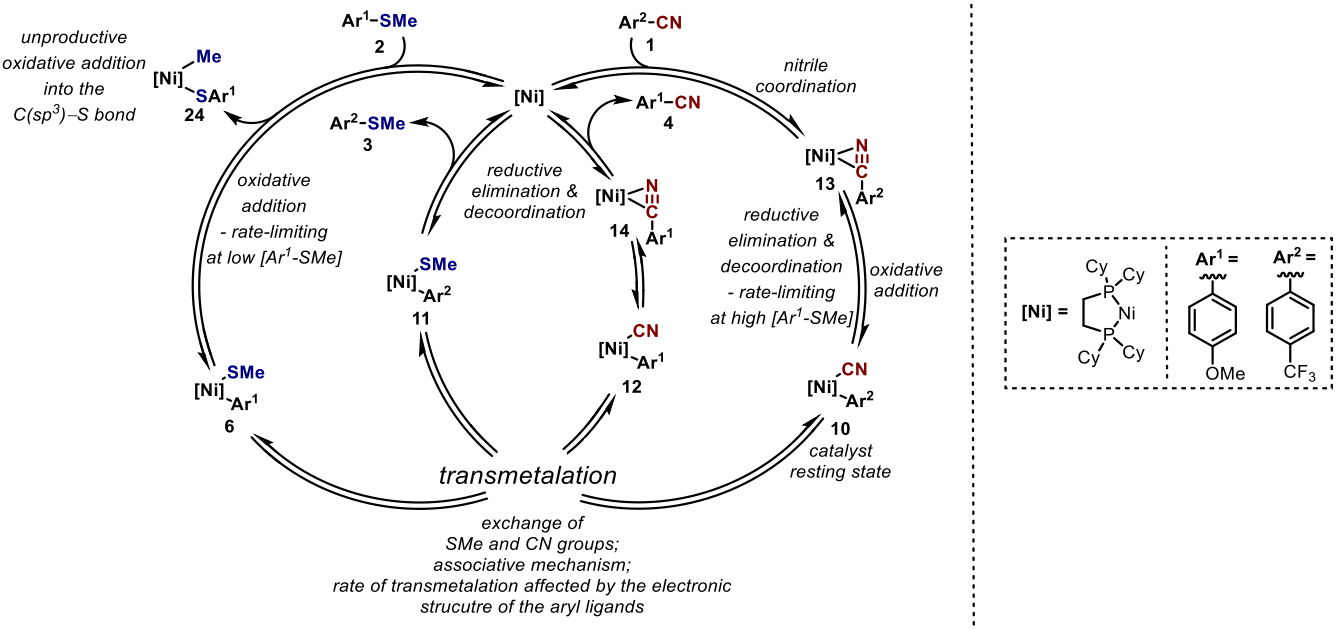

## CONCLUSION

By combining advanced *in situ* NMR spectroscopy, stoichiometric organometallic reactions with putative catalytic intermediates, kinetic analysis, and computational studies, we were able to shed light on the mechanism of the nickel-catalyzed functional group metathesis between aryl sulfides and aryl nitriles and answer key questions.

- A mechanism proceeding *via* migratory insertion of the aryl nitrile C≡N bond into the Ni–Ar bond, followed by β-carbon elimination was ruled out. In contrast, a mechanism proceeding through parallel oxidative addition into both the C–CN bond of the aryl nitrile and the C($sp^2$)–S bond of the aryl methyl sulfide, followed by transmetalation and reductive elimination to release the two scrambled products emerged as the most consistent mechanistic hypothesis based on the data obtained.
- We determined by kinetic analysis and NMR spectroscopy that [Ni(dcype)($ArCF_3$)(CN)] (**10**) is the catalyst resting state of the reaction. Eyring plots of all elementary steps, as well as determination of orders in catalyst and reagents revealed that, depending on the concentration of aryl methyl sulfide **2**, either oxidative addition of the nickel catalyst into the C($sp^2$)–S bond of **2** or reductive elimination/decoordination of aryl nitrile **1** are the turnover-limiting steps of the metathesis reaction.
- We propose an associative transition state for the transmetalation between two nickel(II) centers based on Eyring and Hammett studies. *In situ* NMR spectroscopy showed that transmetalation already occurs at temperatures as low as 60 °C.
- By labeling the backbone of the dcype ligand, it was possible to show that the transmetalation occurs *via* exchange of the SMe and the CN ligands, rather than exchange of the aryl groups in 1,2-difluorobenzene. The preferred exchange of the X-type ligands over the aryl groups further explains the absence of biaryl side-products under the reaction conditions, which is an indication that the same may be true for the catalytic conditions.
- A catalyst deactivation pathway *via* oxidative addition into the C($sp^3$)–S bond of the aryl methyl sulfide and subsequent ligand exchange has been identified, which explains the presence of diaryl sulfides as side-product. By varying the sterics of the alkyl substituent on the aryl sulfide, this catalyst deactivation process could be successfully suppressed and the catalyst loading could be halved.

These conclusions should provide a general foundation for the understanding of functional group metathesis reactions and the development of new reactions. We believe the detailed studies of the transmetalation step will have broader implications for the field of nickel catalysis.

## ASSOCIATED CONTENT

**Supporting Information**. Experimental Procedures, spectral and crystallographic data. This material is available free of charge *via* the Internet at http://pubs.acs.org.

## AUTHOR INFORMATION


### Corresponding Author

**Bill Morandi** − *Laboratorium für Organische Chemie, ETH Zürich, 8093 Zürich, Switzerland;* orcid.org/0000-0003-3968-1424; Email: bill.morandi@org.chem.ethz.ch

### Authors

**Philip Boehm** – *Laboratorium für Organische Chemie, ETH Zürich, 8093 Zürich, Switzerland*; orcid.org/0000-0002-9171-4636
**Patrick Müller** − *Laboratorium für Organische Chemie, ETH Zürich, 8093 Zürich, Switzerland;* orcid.org/0000-0001-7253-7198
**Patrick Finkelstein** − *Laboratorium für Organische Chemie, ETH Zürich, 8093 Zürich, Switzerland;* orcid.org/0000-0002-5881-3499
**Miguel A. Rivero-Crespo**− *Laboratorium für Organische Chemie, ETH Zürich, 8093 Zürich, Switzerland*; orcid.org/0000-0003-3968-1424
**Marc-Olivier Ebert** − *Laboratorium für Organische Chemie, ETH Zürich, 8093 Zürich, Switzerland*; orcid.org/0000-0003-1507-219X
**Nils Trapp** − *Laboratorium für Organische Chemie, ETH Zürich, 8093 Zürich, Switzerland*; orcid.org/0000-0002-9075-3967

### Author Contributions

‡These authors contributed equally.



### Funding Sources

The Swiss National Science Foundation (SNSF 184658), the European Research Council (Shuttle Cat, Project ID: 757608), the FCI (scholarship to P.B.) and ETH Zürich are acknowledged for financial support. M.A.R.-C. thanks the Fundacion Ramón Areces for a fellowship. This publication was created as part of NCCR Catalysis, a National Centre of Competence in Research funded by the Swiss National Science Foundation.


### Notes

The authors declare no competing financial interest.


## ACKNOWLEDGMENT

We acknowledge the NMR service and Bruker (Dr. Barbara Czarniecki) for the assistance with (high-temperature) NMR measurements. We thank the Molecular and Biomolecular Analysis Service (MoBiAS) and the X-ray service (SMoCC) for technical assistance. We further thank the whole Morandi group for fruitful discussions and critical proofreading of the manuscript.

## REFERENCES


(1) Grubbs, R. H. *Handbook of Metathesis*; Wiley, 2003. https://doi.org/10.1002/9783527619481.
(2) Hoveyda, A. H.; Zhugralin, A. R. The Remarkable Metal-Catalysed Olefin Metathesis Reaction. *Nature* **2007**, *450*, 243–251. https://doi.org/10.1038/nature06351.
(3) Connon, S. J.; Blechert, S. Recent Developments in Olefin Cross-Metathesis. *Angew. Chem. Int. Ed*. **2003**, *42*, 1900–1923. https://doi.org/10.1002/anie.200200556.
(4) Schrock, R. R.; Hoveyda, A. H. Molybdenum and Tungsten Imido Alkylidene Complexes as Efficient Olefin-Metathesis Catalysts. *Angew. Chem. Int. Ed*. **2003**, *42*, 4592–4633. https://doi.org/10.1002/anie.200300576.
(5) Grela, K. *Olefin Metathesis: Theory and Practice*; Wiley Blackwell, 2014. https://doi.org/10.1002/9781118711613.
(6) Fürstner, A. Olefin Metathesis and Beyond. *Angew. Chem. Int. Ed*. **2000**, *39*, 3012–3043. https://doi.org/10.1002/1521-3773(20000901)39:17<3012::AID-ANIE3012>3.0.CO;2-G
(7) Cossy, J.; Arseniyadis, S.; Meyer, C. *Metathesis in Natural Product Synthesis: Strategies, Substrates and Catalysts*; Wiley-VCH, 2010. https://doi.org/10.1002/9783527629626.
(8) Lecourt, C.; Dhambri, S.; Allievi, L.; Sanogo, Y.; Zeghbib, N.; Ben Othman, R.; Lannou, M. I.; Sorin, G.; Ardisson, J. Natural Products and Ring-Closing Metathesis: Synthesis of Sterically Congested Olefins. *Nat. Prod. Rep.* **2018**, *35*, 105–124. https://doi.org/10.1039/c7np00048k.
(9) Ivin, K. J.; Mol, J. C. Olefin Metathesis and Metathesis Polymerization; Elsevier, 1997.
(10) Grubbs, R. H.; Carr, D. D.; Hoppin, C.; Burk, P. L. Consideration of the Mechanism of the Metal Catalyzed Olefin Metathesis Reaction. *J. Am. Chem. Soc*. **1976**, *98*, 3478–3483. https://doi.org/10.1021/ja00428a015.
(11) Katz, T. J.; McGinnis, J. The Mechanism of the Olefin Metathesis Reaction. *J. Am. Chem. Soc*. **1975**, *97*, 1592–1594. https://doi.org/10.1021/ja00839a063.
(12) Chauvin, Y. Olefin Metathesis: The Early Days (Nobel Lecture). *Angew. Chem. Int. Ed*. **2006**, *45*, 3740–3747. https://doi.org/10.1002/anie.200601234.
(13) Bhawal, B. N.; Morandi, B. Catalytic Isofunctional Reactions—Expanding the Repertoire of Shuttle and Metathesis Reactions. *Angew. Chem. Int. Ed*. **2019**, *58*, 10074–10103. https://doi.org/10.1002/anie.201803797.
(14) De La Higuera Macias, M.; Arndtsen, B. A. Functional Group Transposition: A Palladium-Catalyzed Metathesis of Ar-X σ-Bonds and Acid Chloride Synthesis. *J. Am. Chem. Soc*. **2018**, *140*, 10140–10144. https://doi.org/10.1021/jacs.8b06605.
(15) Lee, Y. H.; Morandi, B. Metathesis-Active Ligands Enable a Catalytic Functional Group Metathesis between Aroyl Chlorides and Aryl Iodides. *Nat. Chem.* **2018**, *10*, 1016–1022. https://doi.org/10.1038/s41557-018-0078-8.
(16) Isshiki, R.; Inayama, N.; Muto, K.; Yamaguchi, J. Ester Transfer Reaction of Aromatic Esters with Haloarenes and Arenols by a Nickel Catalyst. *ACS Catal.* **2020**, *10*, 3490–3494. https://doi.org/10.1021/acscatal.0c00291.
(17) Isshiki, R.; Kurosawa, M. B.; Muto, K.; Yamaguchi, J. Ni-Catalyzed Aryl Sulfide Synthesis through an Aryl Exchange Reaction. *J. Am. Chem. Soc*. **2021**, *143*, 10333–10340. https://doi.org/10.1021/jacs.1c04215.
(18) Delcaillau, T.; Boehm, P.; Morandi, B. Nickel-Catalyzed Reversible Functional Group Metathesis between Aryl Nitriles and Aryl Thioethers. *J. Am. Chem. Soc.* **2021**, *143*, 3723–3728. https://doi.org/10.1021/jacs.1c00529.
(19) Ackerman, L. K. G.; Lovell, M. M.; Weix, D. J. Multimetallic Catalysed Cross-Coupling of Aryl Bromides with Aryl Triflates. *Nature* **2015**, *524*, 454–457. https://doi.org/10.1038/nature14676.
(20) Durak, L. J.; Lewis, J. C. Iridium-Promoted, Palladium-Catalyzed Direct Arylation of Unactivated Arenes. *Organometallics* **2014**, *33*, 620–623. https://doi.org/10.1021/om401221v.
(21) Chan, N. H.; Gair, J. J.; Roy, M.; Qiu, Y.; Wang, D. S.; Durak, L. J.; Chen, L.; Filatov, A. S.; Lewis, J. C. Insight into the Scope and Mechanism for Transmetalation of Hydrocarbyl Ligands on Complexes Relevant to C-H Activation. *Organometallics* **2021**, *40*, 6–10. https://doi.org/10.1021/acs.organomet.0c00628.
(22) Lee, S. Y.; Hartwig, J. F. Palladium-Catalyzed, Site-Selective Direct Allylation of Aryl C-H Bonds by Silver-Mediated C-H Activation: A Synthetic and Mechanistic Investigation. *J. Am. Chem. Soc.* **2016**, *138*, 15278–15284. https://doi.org/10.1021/jacs.6b10220.
(23) Yamamoto, T.; Morita, A.; Miyazaki, Y.; Maruyama, T.; Wakayama, H.; Zhou, Z. hua; Nakamura, Y.; Kanbara, T.; Sasaki, S.; Kubota, K. Preparation of π-Conjugated Poly(Thiophene-2,5-Diyl), Poly(p-Phenylene), and Related Polymers Using Zerovalent Nickel Complexes. Linear Structure and Properties of the π-Conjugated Polymers. *Macromolecules* **1992**, *25*, 1214–1223. https://doi.org/10.1021/ma00030a003.
(24) Yamamoto, T.; Maruyama, T.; Zhou, Z. H.; Ito, T.; Fukuda, T.; Yoneda, Y.; Begum, F.; Ikeda, T.; Sasaki, S.; Takezoe, H.; Fukuda, A.; Kubota, K. φ-Conjugated Poly(Pyridine-2,5-Diyl), Poly(2,2'-Bipyridine-5,5'-Diyl), and Their Alkyl Derivatives. Preparation, Linear Structure, Function as a Ligand to Form Their Transition Metal Complexes, Catalytic Reactions, n-Type Electrically Conducting Properties, Optical Properties, and Alignment on Substrates. *J. Am. Chem. Soc.* **1994**, *116*, 4832–4845. https://doi.org/10.1021/ja00090a031.
(25) Yamamoto, T.; Zhou, Z. H.; Kanbara, T.; Shimura, M.; Kizu, K.; Maruyama, T.; Nakamura, Y.; Fukuda, T.; Lee, B. L.; Ooba, N.; Tomaru, S.; Kurihara, T.; Kaino, T.; Kubota, K.; Sasaki, S. π-Conjugated Donor-Acceptor Copolymers Constituted of π-Excessive and π-Deficient Arylene Units. Optical and Electrochemical Properties in Relation to CT Structure of the Polymer. *J. Am. Chem. Soc.* **1996**, *118*, 10389–10399. https://doi.org/10.1021/ja961550t.
(26) Pérez-Temprano, M. H.; Casares, J. A.; Espinet, P. Bimetallic Catalysis Using Transition and Group 11 Metals: An Emerging Tool for C-C Coupling and Other Reactions. *Chem. Eur. J.* **2012**, *18*, 1864–1884. https://doi.org/10.1002/chem.201102888.
(27) For related recent reports on transmetalation between two Pd centers, see: Kristensen, S. K.; Eikeland, E. Z.; Taarning, E.; Lindhardt, A. T.; Skrydstrup, T. Ex Situ Generation of Stoichiometric HCN and Its Application in the Pd-Catalysed Cyanation of Aryl Bromides: Evidence for a Transmetallation Step between Two Oxidative Addition Pd-Complexes. *Chem. Sci.* **2017**, *8*, 8094–8105. https://doi.org/10.1039/c7sc03912c.
(28) Casado, A. L.; Casares, J. A.; Espinet, P. An Aryl Exchange Reaction with Full Retention of Configuration of the Complexes: Mechanism of the Aryl Exchange between $[PdR_2L_2]$ Complexes in Chloroform (R = Pentahalophenyl, L = Thioether). *Organometallics* **1997**, *16*, 5730–5736. https://doi.org/10.1021/om970721f.
(29) Tan, Y.; Barrios-Landeros, F.; Hartwig, J. F. Mechanistic Studies on Direct Arylation of Pyridine N -Oxide: Evidence for Cooperative Catalysis between Two Distinct Palladium Centers. *J. Am. Chem. Soc.* **2012**, *134*, 3683–3686. https://doi.org/10.1021/ja2122156.
(30) Wang, D.; Izawa, Y.; Stahl, S. S. Pd-Catalyzed Aerobic Oxidative Coupling of Arenes: Evidence for Transmetalation between Two Pd(II)-Aryl Intermediates. *J. Am. Chem. Soc.* **2014**, *136*, 9914–9917. https://doi.org/10.1021/ja505405u.
(31) Kim, J.; Hong, S. H. Ligand-Promoted Direct C-H Arylation of Simple Arenes: Evidence for a Cooperative Bimetallic Mechanism. *ACS Catal.* **2017**, *7*, 3336–3343. https://doi.org/10.1021/acscatal.7b00397.

(32) Kim, D.; Choi, G.; Kim, W.; Kim, D.; Kang, Y. K.; Hong, S. H. The Site-Selectivity and Mechanism of Pd-Catalyzed C($sp^2$)–H Arylation of Simple Arenes. *Chem. Sci.* **2021**, *12*, 363–373. https://doi.org/10.1039/D0SC05414C.
(33) Gazvoda, M.; Virant, M.; Pinter, B.; Košmrlj, J. Mechanism of Copper-Free Sonogashira Reaction Operates through Palladium-Palladium Transmetallation. *Nat. Commun.* **2018**, *9*, 4814. https://doi.org/10.1038/s41467-018-07081-5.
(34) Tsou, T. T.; Kochi, J. K. Mechanism of Biaryl Synthesis with Nickel Complexes. *J. Am. Chem. Soc.* **1979**, *101*, 7547–7560. https://doi.org/10.1021/ja00519a015.
(35) Yamamoto, T.; Wakabayashi, S.; Osakada, K. Mechanism of C–C Coupling Reactions of Aromatic Halides, Promoted by $Ni(COD)_2$ in the Presence of 2,2′-Bipyridine and $PPh_3$, to Give Biaryls. *J. Organomet. Chem.* **1992**, *428*, 223–237. https://doi.org/10.1016/0022-328X(92)83232-7.
(36) Yamamoto, T.; Abla, M.; Murakami, Y. Promotion of Reductive Elimination Reaction of Diorgano(2,2′-Bipyridyl)Nickel(II) Complexes by Electron-Accepting Aromatic Compounds, Lewis Acids, and Brønsted Acids. *Bull. Chem. Soc. Jpn.* **2002**, *75*, 1997–2009. https://doi.org/10.1246/bcsj.75.1997.
(37) Poisson, P.-A.; Tran, G.; Besnard, C.; Mazet, C. Nickel-Catalyzed Kumada Vinylation of Enol Phosphates: A Comparative Mechanistic Study. *ACS Catal.* **2021**, 15041–15050. https://doi.org/10.1021/ACSCATAL.1C04800.
(38) For related work on bimetallic reductive elimination from nickel, see: Xu, H.; Diccianni, J. B.; Katigbak, J.; Hu, C.; Zhang, Y.; Diao, T. Bimetallic C-C Bond-Forming Reductive Elimination from Nickel. *J. Am. Chem. Soc.* **2016**, *138*, 4779–4786. https://pubs.acs.org/doi/10.1021/jacs.6b00016.
(39) Ansyln, E. V.; Dougherty D. A. *Modern Physical Organic Chemistry*; University Science Books, 2006.
(40) Delcaillau, T.; Bismuto, A.; Lian, Z.; Morandi, B. Nickel-Catalyzed Inter- and Intramolecular Aryl Thioether Metathesis by Reversible Arylation. *Angew. Chem. Int. Ed.* **2020**, *59*, 2110–2114. https://doi.org/10.1002/anie.201910436.
(41) Bismuto, A.; Delcaillau, T.; Müller, P.; Morandi, B. Nickel-Catalyzed Amination of Aryl Thioethers: A Combined Synthetic and Mechanistic Study. *ACS Catal.* **2020**, *10*, 4630–4639. https://doi.org/10.1021/acscatal.0c00393.
(42) Wong, Y. C.; Parthasarathy, K.; Cheng, C. H. Direct Synthesis of Arylketones by Nickel-Catalyzed Addition of Arylboronic Acids to Nitriles. *Org. Lett.* **2010**, *12*, 1736–1739. https://doi.org/10.1021/ol1003252.
(43) Hsieh, J. C.; Chen, Y. C.; Cheng, A. Y.; Tseng, H. C. Nickel-Catalyzed Intermolecular Insertion of Aryl Iodides to Nitriles: A Novel Method to Synthesize Arylketones. *Org. Lett.* **2012**, *14*, 1282–1285. https://doi.org/10.1021/ol300153f.
(44) For a related stoichiometric study on migratory insertions into nitriles with Rhodium, see: Zhao, P.; Hartwig, J. F. Insertions of Ketones and Nitriles into Organorhodium(I) Complexes and β-Hydrocarbyl Eliminations from Rhodium(I) Alkoxo and Iminyl Complexes. *Organometallics* **2008**, *27*, 4749–4757. https://doi.org/10.1021/om800378v.
(45) Zhao, P.; Hartwig, J. F. β-Aryl Eliminations from Rh(I)-Iminyl Complexes. *J. Am. Chem. Soc.* **2005**, *127*, 11618–11619. https://doi.org/10.1021/ja054132.
(46) Zhao, P.; Incarvito, C. D.; Hartwig, J. F. Direct Observation of β-Aryl Eliminations from Rh(I) Alkoxides. *J. Am. Chem. Soc.* **2006**, *128*, 3124–3125. https://doi.org/10.1021/ja058550q.
(47) Malapit, C. A.; Reeves, J. T.; Busacca, C. A.; Howell, A. R.; Senanayake, C. H. Rhodium-Catalyzed Transnitrilation of Aryl Boronic Acids with Dimethylmalononitrile. *Angew. Chem. Int. Ed.* **2016**, *55*, 326–330. https://doi.org/10.1002/anie.201508122.
(48) Tobisu, M.; Kinuta, H.; Kita, Y.; Rémond, E.; Chatani, N. Rhodium(I)-Catalyzed Borylation of Nitriles through the Cleavage of Carbon-Cyano Bonds. *J. Am. Chem. Soc.* **2012**, *134*, 115–118. https://doi.org/10.1021/ja2095975.
(49) Esteruelas, M. A.; Oliván, M.; Vélez, A. Conclusive Evidence on the Mechanism of the Rhodium-Mediated Decyanative Borylation. *J. Am. Chem. Soc.* **2015**, *137*, 12321–12329. https://doi.org/10.1021/jacs.5b07357.
(50) Jiang, Y. Y.; Yu, H. Z.; Fu, Y. Mechanistic Study of Borylation of Nitriles Catalyzed by Rh-B and Ir-B Complexes via C-CN Bond Activation. *Organometallics* **2013**, *32*, 926–936. https://doi.org/10.1021/om301263s.
(51) Lutz, M. D. R.; Morandi, B. Metal-Catalyzed Carbon-Carbon Bond Cleavage of Unstrained Alcohols. *Chem. Rev.*. **2021**, *121*, 300–326. https://doi.org/10.1021/acs.chemrev.0c00154.
(52) Mills, L. R.; Graham, J. M.; Patel, P.; Rousseaux, S. A. L. Ni-Catalyzed Reductive Cyanation of Aryl Halides and Phenol Derivatives via Transnitrilation. *J. Am. Chem. Soc.* **2019**, *141*, 19257–19262. https://doi.org/10.1021/jacs.9b11208.
(53) Garcia, J. J.; Brunkan, N. M.; Jones, W. D. Cleavage of Carbon-Carbon Bonds in Aromatic Nitriles Using Nickel(0). *J. Am. Chem. Soc.* **2002**, *124*, 9547–9555. https://doi.org/10.1021/ja0204933.
(54) Ateşin, T. A.; Li, T.; Lachaize, S.; García, J. J.; Jones, W. D. Experimental and Theoretical Examination of C-CN Bond Activation of Benzonitrile Using Zerovalent Nickel. *Organometallics* **2008**, *27*, 3811–3817. https://doi.org/10.1021/om800424s.
(55) Li, T.; García, J. J.; Brennessel, W. W.; Jones, W. D. C-CN Bond Activation of Aromatic Nitriles and Fluxionality of the $\eta^2$-Arene Intermediates: Experimental and Theoretical Investigations. *Organometallics* **2010**, *29*, 2430–2445. https://doi.org/10.1021/om100001m.
(56) As the metathesis between aryl thioethers and aryl nitriles works equally well in toluene-$d_8$, compared to o-xylene-$d_{10}$ and especially after we realized that the $^{31}P\{^1H\}$ NMR spectra of the catalytic reaction in both solvents were identical, we decided to use toluene-$d_8$ instead of the more expensive and less available o-xylene-$d_{10}$ in our study.
(57) Blackmond, D. G. Reaction Progress Kinetic Analysis: A Powerful Methodology for Mechanistic Studies of Complex Catalytic Reactions. *Angew. Chem. Int. Ed.* **2005**, *44*, 4302–4320. https://doi.org/10.1002/anie.200462544.
(58) Blackmond, D. G. Kinetic Profiling of Catalytic Organic Reactions as a Mechanistic Tool. *J. Am. Chem. Soc.* **2015**, *137*, 10852–10866. https://doi.org/10.1021/jacs.5b05841.
(59) Neese, F. The ORCA Program System. *WIREs Computational Molecular Science* **2012**, *2*, 73–78. https://doi.org/10.1002/wcms.81
(60) Neese, F. Software Update: The ORCA Program System, Version 4.0. *WIREs Computational Molecular Science* **2018**, *8* (1), e1327. https://doi.org/10.1002/wcms.1327.
(61) Becke, A. D. Density-Functional Exchange-Energy Approximation with Correct Asymptotic Behavior. *Phys. Rev. A* **1988**, *38*, 3098–3100. https://doi.org/10.1103/PhysRevA.38.3098.
(62) Perdew, J. P. Density-Functional Approximation for the Correlation Energy of the Inhomogeneous Electron Gas. *Phys. Rev. B* **1986**, *33*, 8822–8824. https://doi.org/10.1103/PhysRevB.33.8822.
(63) Weigend, F.; Ahlrichs, R. Balanced Basis Sets of Split Valence, Triple Zeta Valence and Quadruple Zeta Valence Quality for H to Rn: Design and Assessment of Accuracy. *Phys. Chem. Chem. Phys.* **2005**, *7*, 3297–3305. https://doi.org/10.1039/B508541A.
(64) Grimme, S.; Antony, J.; Ehrlich, S.; Krieg, H. A Consistent and Accurate Ab Initio Parametrization of Density Functional Dispersion Correction (DFT-D) for the 94 Elements H-Pu. *J. Chem. Phys.* **2010**, *132*, 154104. https://doi.org/10.1063/1.3382344.
(65) Grimme, S.; Ehrlich, S.; Goerigk, L. Effect of the Damping Function in Dispersion Corrected Density Functional Theory. *J. Comput. Chem.* **2011**, *32*, 1456–1465. https://doi.org/10.1002/jcc.21759.

(66) Adamo, C.; Barone, V. Toward Reliable Density Functional Methods without Adjustable Parameters: The PBE0 Model. *J. Chem. Phys.* **1999**, *110*, 6158–6170. https://doi.org/10.1063/1.478522.
(67) Harris, R. K.; Mann, B. E. *NMR and the Periodic Table*; Academic Press, 1978; pp 107–122.
(68) Cámpora, J.; Matas, I.; Palma, P.; Graiff, C.; Tiripicchio, A. Fluoride Displacement by Lithium Reagents. An Improved Method for the Synthesis of Nickel Hydroxo, Alkoxo, and Amido Complexes. *Organometallics* **2005**, *24*, 2827–2830. https://doi.org/10.1021/om0489709.
(69) Cámpora, J.; Matase, I.; Palma, P.; Álvarez, E.; Graiff, C.; Tiripicchio, A. Monomeric Alkoxo and Amido Methylnickel(II) Complexes. Synthesis and Heterocumulene Insertion Chemistry. *Organometallics* **2007**, *26*, 3840–3849. https://doi.org/10.1021/om7002909.
(70) Ariyananda, P. W. G.; Kieber-Emmons, M. T.; Yap, G. P. A.; Riordan, C. G. Synthetic Analogs for Evaluating the Influence of N-H···S Hydrogen Bonds on the Formation of Thioester in Acetyl Coenzyme a Synthase. *Dalt. Trans.* **2009**, 4359–4369. https://doi.org/10.1039/b901192g.
(71) Desnoyer, A. N.; Friese, F. W.; Chiu, W.; Drover, M. W.; Patrick, B. O.; Love, J. A. Exploring Regioselective Bond Cleavage and Cross-Coupling Reactions Using a Low-Valent Nickel Complex. *Chem. Eur. J.* **2016**, *22*, 4070–4077. https://doi.org/10.1002/chem.201504959.
(72) Hua, R.; Takeda, H.; Onozawa, S. Y.; Abe, Y.; Tanaka, M. Nickel-Catalyzed Thioallylation of Alkynes with Allyl Phenyl Sulfides. *Org. Lett.* **2007**, *9*, 263–266. https://doi.org/10.1021/ol062686r.
(73) Sgro, M. J.; Stephan, D. W. Oxidative Addition Reactions of Bis-Aminophosphine and Bis-Phosphinite Nickel(0) Pincer Complexes. *Organometallics* **2012**, *31*, 1584–1587. https://doi.org/10.1021/om201229x.
(74) Matsunaga, P. T.; Hillhouse, G. L. Thianickelacycles by Ring-Opening Reactions of Cyclic Thioethers and Their Subsequent Carbonylation to Thioesters. *Angew. Chem. Int. Ed.* **1994**, *33*, 1748–1749. https://doi.org/10.1002/anie.199417481.

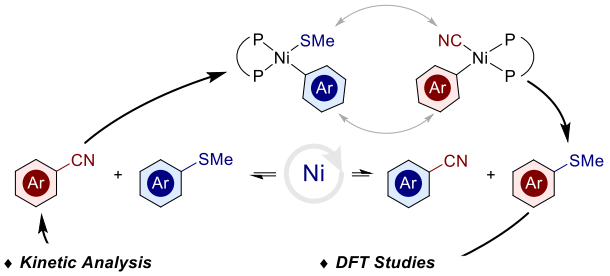


- *Kinetic Analysis*
- *Eyring and Hammett Plots*
- *> 30 new Ni complexes isolated*
- *DFT Studies*
- *Deuterium-labelling Experiments*
- *Improved Catalytic Protocol*